http://dx.doi.org/10.1080/10255842.2012.693173

Subject-specific musculoskeletal model of the lower limb in a lying and standing position

J. Hausselle[a]*, A. Assi[a], A. El Helou[a], E. Jolivet[a], H. Pillet[a], E. Dion[b], D. Bonneau[a] and W. Skalli[a]

[a] *LBM, Arts et Metiers ParisTech, Paris, France;* [b]*Service d'Imagerie Me´dicale, AP-HP, Ho^pital Louis Mourier, Colombes, France*

Accurate estimation of joint loads implies using subject-specific musculoskeletal models. Moreover, as the lines of action of the muscles are dictated by the soft tissues, which are in turn influenced by gravitational forces, we developed a method to build subject-specific models of the lower limb in a functional standing position. Bones and skin envelope were obtained in a standing position, whereas muscles and a set of bony landmarks were obtained from conventional magnetic resonance images in a lying position. These muscles were merged with the subject-specific skeletal model using a nonlinear transformation, taking into account soft tissue movements and gravitational effects. Seven asymptomatic lower limbs were modelled using this method, and results showed realistic deformations. Comparing the subject-specific skeletal model to a scaled reference model rendered differences in terms of muscle length up to 4% and in terms of moment arm for adductor muscles up to 30%. These preliminary findings enlightened the importance of subject-specific modelling in a functional position.

Keywords: modelling; subject specific; muscles; nonlinear deformation; muscular parameters

1. Introduction

Three-dimensional musculoskeletal models of the lower limbs are widely used for gait simulation and are needed to compute joint loads (Delp et al. 1990; Eredmir et al. 2007). Muscular parameters required to estimate joint muscle forces include muscle–tendon length, moment arm length and maximal cross-sectional area (Redl et al. 2007; Scheys et al. 2008). Lately, there has been an increased concern about the accuracy of such models, usually obtained by rescaling a reference model through anthropometric measurements (Delp et al. 1990; Delp and Loan, 1995; Heller et al. 2001). This scaling method can lead to inaccuracies concerning muscle paths and therefore moment arms (Scheys et al. 2008). These inaccuracies justify the importance of subject-specific musculoskeletal models using medical images (Blemker et al. 2005) and in particular magnetic resonance imaging (MRI) (Scheys et al. 2009). Because of manual contouring, 3D muscle reconstruction from a full set of MR images is time consuming, which limits its extensive use.

A novel fast reconstruction method has been recently proposed for building subject-specific muscular models by contouring a reduced set of MR images (Assi et al. 2008; Jolivet et al. 2008; Südhoff et al. 2009). Although muscular geometries obtained are accurate, MR images are usually taken in a lying position, implying potential geometrical changes in muscle geometries when shifted to a standing position. These changes are mainly due to gravitational effect on soft tissues, but also due to postural changes between these two positions. Moreover, in the case of abnormal bone deformities, the posture can dramatically change between the lying and standing position, thus increasing the inaccuracy introduced by using MR images in one position and a reference model in the other (Scheys et al. 2011).

The first aim of this study was to assess the feasibility of building subject-specific musculoskeletal models based on both MR and biplanar X-ray images, taking into account changes in relative bone position and muscle shape between lying (MRI) and standing (X-rays) positions. The second goal was to assess the sensitivity of the standing subject-specific model with respect to the number of control points used for the deformation procedure. Finally, the third goal was to compare muscle lengths and moment arms to those obtained using a scaled reference model.

2. Materials and methods

The overall strategy was to use the bony landmarks obtained in the lying position to register the 'lying' skin envelope on the standing skeletal model. With both skin envelopes in the standing configuration, a nonlinear transformation was then defined, which links the registered 'lying' skin envelope with the 'standing' envelope. The muscle models obtained in the lying position were then registered and deformed using the same transformation, thus enabling us to compare lengths and moment arms between registered and registered + deformed muscles.

*Corresponding author. Email: jerome.hausselle@gmail.com

2.1 Subjects

Four asymptomatic young men [age 27 ± 4 years, height 181 ± 2 cm, weight 75 ± 15 kg and body mass index (BMI) 23 ± 4] consented to participate in the protocol previously approved by institutional ethics committees. Seven lower limbs were finally selected, as one could not be used because of insufficient skin envelope visible on the X-ray images.

2.2 Skeletal model and associated skin envelope

We used a biplanar X-ray system (EOS®, Biospace Med, Paris, France) to acquire X-ray images of subjects in a standing position (Dubousset et al. 2005, coll. LBM, Arts et Metiers ParisTech, France, LIO, ETS-CRCHUM, Canada, Biospace Med, Paris, France and Saint Vincent de Paul Hospital, France). The 3D geometry of the lower limbs was obtained using a specific reconstruction software based on Morphorealistic Parametric Subject Specific Model (Baudouin et al. 2008; Chaibi et al. 2012). The model also included insertion points of 22 lower limb muscles (Table 1). The skin envelopes of the lower limbs were also reconstructed using the Non Stereo Corresponding Contours method (Laporte et al. 2003). Furthermore, we used anatomical landmarks to define the local coordinate system for each bone.

The skeletal models obtained in the global X-ray coordinate system thus included the local coordinate systems, the Virtual Reality Modeling Language (VRML) objects modelling the 3D bones, the skin envelope and the 2×22 muscle insertion points (Figure 1(a)):

- Nodes of the bones were noted $\{B_j\}_i$, with $i = 1, \ldots, 5$ (pelvis, left and right femurs and left and right tibias-fibulas) and j varying between 9300 and 1500, depending on the bone considered.
- Nodes of the skin envelope were noted $\{SX_j\}_i$, with $i = 1, 2$ (left and right) and j varying between 4000 and 3300, depending on the segment considered (hip and thigh or leg).
- Muscle insertion points were noted $\{IX_i\}$, with $i = 1, \ldots, 88$ (22 muscles on each limb with two insertion points per muscle).

Table 1. List of the 22 muscles of the lower limb considered.

Adductor brevis	Iliacus
Adductor longus	Rectus femoris[a]
Adductor magnus	Sartorius[a]
Biceps femoris (long head)[a]	Semimembranosus[a]
Biceps femoris (short head)	Semitendinosus[a]
Gastrocnemius (lateral)[a]	Soleus[a]
Gastrocnemius (medial)[a]	Tensor fasciae latae
Gluteus maximus	Tibialis anterior[a]
Gluteus medius	Vastus intermedius
Gluteus minimus	Vastus lateralis
Gracilis	Vastus medialis

[a] Muscle used for length and shape comparison to the rescaled generic model.

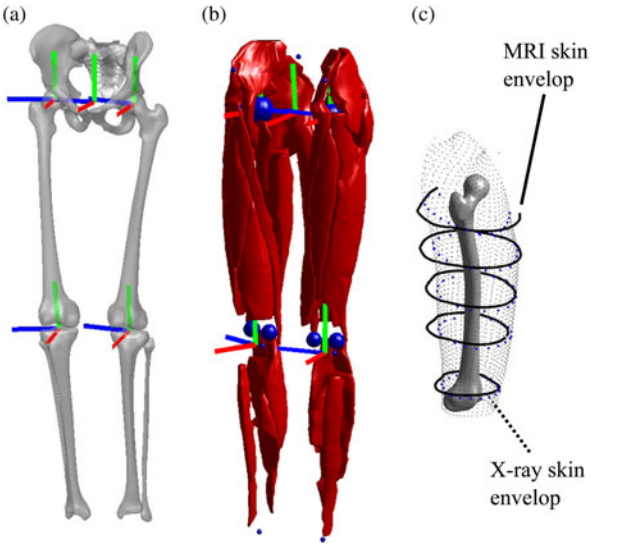

Figure 1. (a) Skeletal model in the standing position, obtained from the biplanar X-ray images reconstruction, with the associated local coordinate system. (b) Muscular model in the lying position, obtained from MR images, with defined anatomical landmarks and the associated local coordinate system. (c) Example of control points $\{CSM_j\}_i$ and $\{CSX_j\}_i$, respectively, defined based on MRI (black lines) and X-ray (blue dots) skin envelopes.

2.3 Muscular model and associated skin envelope

The subjects were scanned using a Philips MRI scanner to obtain axial images, from the iliac crests to the calcaneum (slice thickness: 10 mm; gap: 0 mm; resolution: 0.78×0.78 mm). Geometries of 22 main muscles of each lower limb were reconstructed (Jolivet et al. 2008; Nordez et al. 2009). The external envelope was also reconstructed using the same technique. In addition, 18 anatomical bony landmarks were manually positioned on the MR images in order to define the local coordinate system of each bony segment (Table 2).

The muscular models in the global MRI coordinate system thus included the local coordinate systems of all the bony segments, the VRML objects modelling the 3D geometry of the 2×22 muscles and the skin envelope (Figure 1(b)):

Table 2. Anatomical landmarks of the lower limb defined on the MR images.

Anatomical landmarks	Geometric entity
ASIS	Point
Postero-superior iliac spine	Point
Acetabulum	Sphere
Femoral head	Sphere
Lateral condyle	Sphere
Medial condyle	Sphere
Lateral tibial plateau	Closed spline
Medial tibial plateau	Closed spline
Distal part of the tibia	Closed spline

- Nodes of the muscles were noted $\{M_j\}_i$, with $i = 1, \ldots, 44$ and j varying between 7200 and 500, depending on the muscle considered.
- Nodes of the skin envelope were noted $\{SM_j\}_i$, with $i = 1, 2$ and j varying between 13,000 and 5200, depending on the segment considered (hip and thigh or leg).

2.4 *Muscle deformation between lying and standing positions*

To define and apply a nonlinear transformation, two steps were followed.

The first step was to compute transition matrices between the X-ray and the MRI coordinate systems. We used the local coordinate system of each bone to calculate these matrices (Figure 1), noted $[TM]_i$, with $i = 1, \ldots, 5$ (pelvis, left and right femurs and left and right tibias-fibulas). Using these matrices, muscle insertion points $\{IM\}_i$ for each bone (i) were obtained in the MRI coordinate system as:

$$\{IM_k\} = [TM]_i * \{IX_k\}$$

with $k = 1, \ldots, N$ the number of insertion points on bone (i).

The second step was the definition of the nonlinear deformation (Trochu 1993), based on the transformation between the so-called control points. Two sets of control points were thus defined, one in the MRI coordinate system and another in the X-ray coordinate system. These points were first obtained in the MRI coordinate system:

- For each bony segment, five equally spaced planes were chosen. The MRI control points were then defined as 20 points equally distributed along the intersections of those planes with the skin envelope (Figure 1(c)). The control points obtained were noted $\{CSM_j\}_i$, with $i = 1, \ldots, 5$ and $j = 1, \ldots, 100$. After rigid registration of the planes in the X-ray coordinate system, corresponding X-ray control points were defined as 20 points equally distributed along the intersections of those registered planes with the skin envelope (Figure 1(c)). These points were noted $\{CSX_j\}_i$, again with $i = 1, \ldots, 5$ and $j = 1, \ldots, 100$.
- Muscle insertion control points consisted of muscle insertion points $\{IX_i\}$ and $\{IM_i\}$, with $i = 1, \ldots, 88$, previously defined in each coordinate system.

Therefore, the whole set of control points was defined as:

$$\{CPM_m\} = \bigcup_{i=1}^{5} \{CSM_j\}_i \bigcup \{IM_k\}$$

in the MRI coordinate system

$$\{CPX_m\} = \bigcup_{i=1}^{5} \{CSX_j\}_i \bigcup \{IX_k\}$$

in the X-ray coordinate system

with $m = 588$ for two lower limbs.

The algorithm calculated the transformation which best fitted the MRI control points with the X-ray control points. This transformation was then applied to the nodes $\{M_j\}_i$ of the VRML objects defining the muscle geometries, giving new sets of nodes in the X-ray coordinate system. A post-processing treatment computed muscle volumes before and after kriging deformation and applied a homothetic transformation if the volume difference exceeded 1%.

2.5 *Deformation and muscle parameters*

The number of control points was the key parameter to define the nonlinear deformation. This number depended on two other parameters: the number of MRI slices chosen and the number of control points defined on each intersection of the slice planes with the skin envelope. A sensitivity analysis was carried out for one of the models to assess the influence of these two parameters on the accuracy of the deformation.

The number of slices per bony segment was chosen between 1 and 10, whereas the number of control points per slice was chosen among the following list: 4, 6, 10, 15, 20, 25, 30, 35 and 40. All possible combinations of these two parameters were tested, giving 90 different models of one lower limb. The reference model was the one obtained by using the maximum number of control points, i.e. with 10 slices and 40 points per slice. Each deformed model was compared with the reference model by calculating the root mean square (RMS) error of node-to-node distances for each muscle.

2.6 *Muscle parameters between lying and standing*

The rigidly registered muscles were compared to the deformed muscles by calculating the RMS error of node-to-node distances, in order to assess which muscles were most sensitive to the deformation process.

2.7 *Comparison of a subject-specific musculoskeletal model to a scaled reference model*

A musculoskeletal model of the lower limb, with muscles modelled using via points, was exported from OpenSim 1.8.1 (Delp et al. 1997). We defined the same local coordinate systems as for each of the bone of the subject-specific models. This reference model was then modified to fit the subject-specific model:

- *Isotropic scaling*: the scaling factor was the vertical distance between the antero-superior iliac spine (ASIS) and the centre of the distal part of the tibia, with the hip and knee fully extended.
- Registration of each bone using the corresponding local coordinate system.

The rescaled reference model was therefore in the exact same position of the subject-specific model, i.e. moment arm differences were only due to muscle path definition.

Only fusiform muscles were compared (Table 1). We calculated length difference between the lines of action of 3D and reference muscle for each muscle (Figure 7(a)), using the following steps:

- Definition of a bone of reference.
- Definition of two planes orthogonal to the vertical axis of the local coordinate system of the bone of reference, and delimiting the shortest muscle (3D or reference model).
- Definition of the line of action of the 3D muscle by calculating the barycentre of each slice.
- Definition of 20 via points equally distributed on the line of action of both the 3D and reference muscles, and lying between the upper and lower planes previously defined. These points were noted $\{P_i\}_{3D}$ and $\{P_i\}_G$, respectively.
- Muscle lengths were calculated as the summed distances between consecutive points of $\{P_i\}_{3D}$ and $\{P_i\}_G$.

Muscle moment arms were then calculated in static as the shortest distance between the joint centre and the muscle line of action. The centre of the hip joint was defined as the centre of the sphere fitting the acetabulum, whereas the centre of the knee joint was defined as the midpoint between centres of the least-square spheres fitting the posterior parts of the condyles. Moment arm differences were normalised according to moment arm values of the scaled reference model.

3. Results

The proposed method allowed the definition of subject-specific musculoskeletal systems in a standing position (Figure 2). The modelling process took approximately 20 min for the bones, 1 h 30 min for the muscles and 2 min of computation to deform all the muscles. Therefore, the entire process took less than 2 h to obtain a subject-specific model of one lower limb.

3.1 Deformation and muscle parameters

The RMS error ranged from 0.2 to 8 mm (Figure 3), depending on the two parameters, which were the number of slices per bony segment and the number of control points per slice. The RMS error started to converge with at least 20 points per slice. The most sensitive muscles appeared to be the muscles of the pelvic region, e.g. adductors and gluteii muscles (Figure 4). On the other hand, the RMS error was quite homogeneous for the thigh and leg muscles and lower for the leg.

Figure 2. Example of a subject-specific musculoskeletal model in a standing position.

3.2 Comparison of a subject-specific musculoskeletal model to a scaled reference model

Nine fusiform muscles were considered, for which length differences ranged from 0.2% to 3.6% (Figure 5). The lowest difference was found for the tibialis anterior, whereas the semimembranosus and medial gastrocnemius

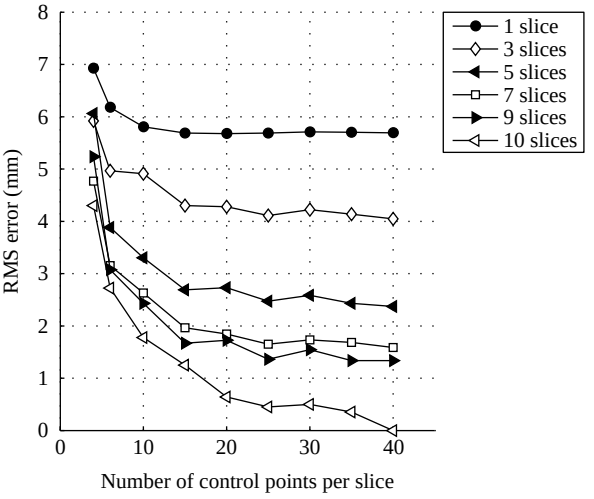

Figure 3. RMS error (mm) for each combination of the two deformation parameters: number of slices and number of control points per slice.

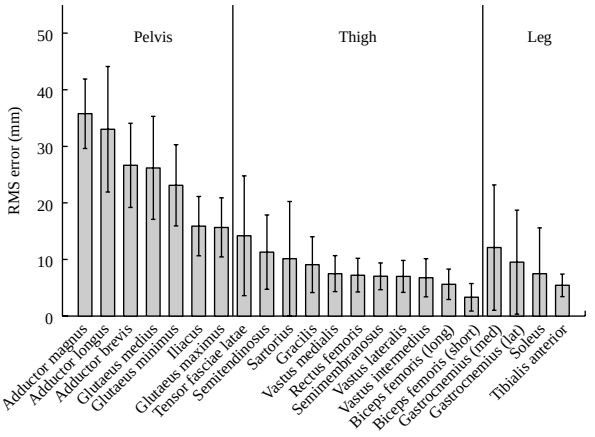

Figure 4. RMS error (mean ± standard deviation (mm)) between registered and registered + deformed muscles, for each bony segment (pelvis, thigh and leg).

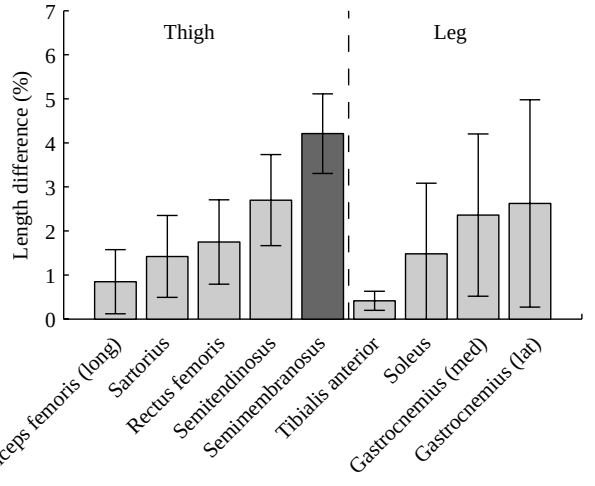

Figure 5. Length differences (mean ± standard deviation (%)) between fusiform muscles of personalised and rescaled reference models.

exhibited a difference exceeding 3%. Moreover, a high inter-individual variation was found for the soleus and lateral gastrocnemius muscles (CV > 90%).

Moment arms of 14 muscles acting at the hip joint were compared to those of the rescaled reference model (Table 3). Nine of the moment arm differences exceeded 10%. In particular, concerning the three adductor muscles, the values obtained with the subject-specific models were lower than those obtained with the rescaled reference model. For the knee joint, moment arms of 11 muscles were assessed, and four showed differences greater than 10%.

4. Discussion

The aim of the proposed method was to develop a subject-specific musculoskeletal model of the lower limb in a standing position. The challenge was to consider soft tissue and relative bone position modifications between the lying and standing configurations, to accurately assess muscle lengths and moment arms in the functional standing position. The method presented here, in addition to MR images, required calibrated biplanar X-ray images.

Muscle deformations could mainly be attributed to soft tissue displacement but also to changes in bone's relative positions. As expected, the most deformed muscles were those of the pelvic region (Figure 4), even though inter-subject variability due to subject's BMI and respective positions during data acquisition was quite high. The changes in this region were expected as, on the one hand, the pelvis's alignment was not preserved between the two positions, and on the other hand, posterior muscles (e.g. gluteii) were flattened when the subject lay on the table in the MRI system. Concerning adductors and iliacus muscles (hip flexors), changes in hip joint configuration would obviously modify their line of action, as flexion was usually more important in the lying position (Figure 6(a)). Gluteii muscles were deformed due to soft tissue movements according to shape changes of the skin envelope between the two positions (Figure 6(b)). Moreover, the complex bone geometry of the pelvis introduced complex muscle geometries as well. Deformations of the thigh muscles were mainly due to soft tissue

Table 3. Mean and standard deviation of lever arm differences (subject-specific – rescaled reference model) for muscles acting around the hip and knee.

	Muscle	Mean (%)	Standard deviation (%)
Hip	Adductor brevis	−34	14
	Adductor longus	−34	6
	Adductor magnus	−28	27
	Gluteus minimus	−25	9
	Sartorius	20	20
	Rectus femoris	15	19
	Gluteus medius	−9	7
	Semimembranosus	−8	6
	Gracilis	−5	5
	Iliacus	−5	32
	Semitendinosus	4	8
	Tensor of fascia latae	4	10
	Gluteus maximus	2	14
	Biceps femoris (long head)	−1	6
Knee	Gracilis	−28	39
	Tensor of fascia latae	18	12
	Semimembranosus	16	39
	Rectus femoris	−14	14
	Biceps femoris (short head)	9	9
	Semitendinosus	7	38
	Vastus intermedius	−7	7
	Vastus medialis	−7	7
	Sartorius	−6	17
	Vastus lateralis	−3	20
	Biceps femoris (long head)	0	12

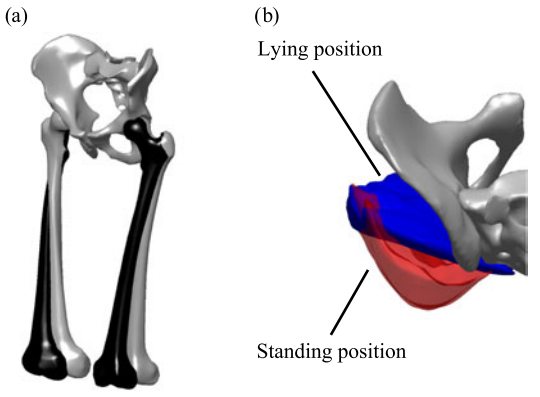

Figure 6. (a) Right and left femur positions in the MRI (black) and X-ray (grey) systems. (b) Example of the gluteus maximus muscle in the lying and standing positions, i.e. before and after deformation (axial view).

movements. Indeed, in the lying position, anterior, medial and lateral muscles flattened because of gravity, whereas posterior muscles flattened because of potential contact of the thigh with the table. This compression was less important than for the gluteii muscles, which can explain the relatively homogeneous RMS error obtained for the thigh muscles. Deformations of the leg muscles were due to a combination of changes in knee and ankle flexion angles and movements of soft tissue. In particular, deformations of the triceps surae muscles could be due to potential contact of the leg with the table.

Comparison of a subject-specific muscoloskeletal model to a scaled reference model showed that length differences between the subject-specific and rescaled reference muscle's lines of action were below 5%. A first source of difference was inaccuracy in muscle insertion point positions. Indeed, even rescaled, the reference bone models did not correctly fit the subject-specific models, leading to inaccuracies concerning bony insertion points.

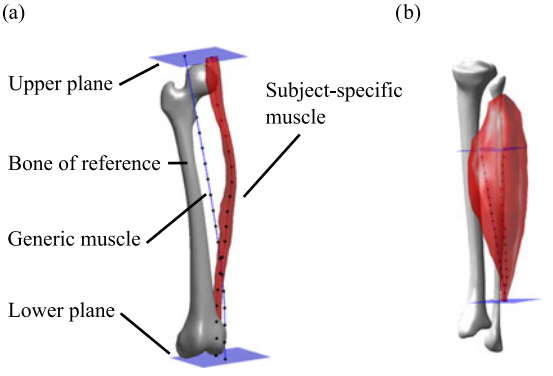

Figure 7. Examples of reference and subject-specific lines of action of sartorius (a) and soleus (b) muscles.

For example, the line of action of the sartorius muscle highly depended on the position of the ASIS (Figure 7(a)), which could be quite different between the two models. For the soleus muscle, differences were mainly due to insertion points definition, chosen on the tibia for the reference model and on the fibula for the subject-specific model (Figure 7(b)).

A second source of differences came from the actual shape of the 3D muscle, which depended on the subject's BMI and its muscular development. This was the case for superficial muscles, as for example the sartorius, which travelled around the rectus femoris and vastus medialis, and the gastrocnemii, which covered the soleus.

Calculations of moment arm differences between subject-specific and rescaled reference models showed that the reference model overestimated moment arms of 9 out of 14 hip muscles, especially concerning adductor muscles (Table 3). Such overestimation has already been found for moment arms (Scheys et al. 2008), but calculations were carried out in dynamics and moment arms were calculated as the first derivative of the change of muscle–tendon length to the joint angle. Moreover, muscles were reconstructed from MR images obtained in a lying position. Concerning muscles crossing the knee joint, moment arms were overestimated for 6 out of 11 of them (Table 3).

MRI-based 3D reconstructions could thus be useful to obtain more accurate muscle paths and to increase the number of via points in reference models. Indeed, Scheys et al. (2009) defined subject-specific muscle paths using an atlas-based non-rigid image registration. The main source of inaccuracy was precisely the use of MR images, taken in a supine position, with the use of a reference model defined in a standing position (Scheys et al. 2011). This study corrected this problem by taking into account joint angle changes between the two positions. A long-term study is to build a database of lower limb models in a standing functional position, which should enable us, for a given subject, to choose the closest model in the database and directly derive the muscle paths from the subject bone geometries and BMI. This type of database could allow using subject-specific models in clinical routine, providing basic inputs such as joint centres and skeletal segment lengths. These inputs could be obtained via functional movements recorded through a motion analysis software (Reinbolt et al. 2005) or estimated using two calibrated biplanar X-rays (Chaibi et al. 2012), the latter method being recommended in case of important bony deformities.

Although this method has so far only been tested on healthy subjects, we expect to find even more muscle paths variations for disabled subjects. Indeed, Scheys et al. (2011) showed large differences between subject-specific and scaled muscle moment arms for children with cerebral palsy. In these cases, bony deformities considerably affect the global posture. Moreover, the joint angle changes between lying and functional standing position should be

even greater than for healthy subjects, thus increasing the relevance and effect of the proposed method.

Future work is therefore needed to test this method with disabled subjects, but also to use the obtained models in dynamics. Indeed, a potential problem may be the number of via points used, as a large number may affect the computational time. A sensitivity analysis should be carried out in order to assess for each muscle the optimal number of via points needed to obtain reliable moment arm values. Moreover, an important issue is the actual muscle paths during contraction. Indeed, the paths calculated in this study will definitely change but we do not know whether they will be closer to straight lines than to curve paths. Although deep muscle paths might become straight, superficial muscle paths would probably not, as they will still overlap deeper muscles and other soft tissues. One solution would be to simulate muscle contraction using finite element modelling and to determine the associated muscle paths; however, this approach requires heavy computations as it involves a lot of contact iterations.

5. Conclusion

The purpose of this study was to obtain 3D subject-specific musculoskeletal models in standing position, assess their sensitivity to the number of control points used for the deformation procedure and compare muscle lengths and moment arms with those of a scaled reference model. We defined a nonlinear deformation, taking into account soft tissue and bone displacements between MRI and X-ray data acquisition. This nonlinear transformation was based on bone relative positions and shape modifications of the limb skin envelope. Comparison of a subject-specific musculoskeletal model to a rescaled reference model showed that differences exist between muscles paths, therefore suggesting the use of subject-specific models defined in functional position. A long-term goal is to build a lower limb database, which will enable a quick and accurate definition of subject-specific models, and therefore improve the accuracy of joint load calculations.

Acknowledgement

The authors would like to thank the Centre National de la Recherche Scientifique (CNRS) for funding this study.

References

Assi A, Ghanem I, Skalli W. 2008. Biomechanical analysis of lower limbs for children with cerebral palsy: Gait analysis and musculo-skeletal modelling. Gait Posture. 28(2): S12–S13.

Baudouin A, Skalli W, de Guise JA, Mitton D. 2008. Parametric subject-specific model for in vivo 3D reconstruction using bi-planar X-rays: Application to the upper femoral extremity. Med Biol Eng Comput. 46(8):799–805.

Blemker S, Pinsky P, Delp S. 2005. A 3D model of muscle reveals the causes of nonuniform strains in the biceps brachii. J Biomech. 38(4):657–665.

Chaibi Y, Cresson T, Aubert B, Hausselle J, Neyret P, Hauger O, de Guise JA, Skalli W. 2012. Fast 3D reconstruction of the lower limb using a parametric model and statistical inferences and clinical measurements calculation from biplanar X-rays. Comput Methods Biomech Biomed Eng. 15(5):457–466.

Delp S, Loan J, Hoy M, Zajac F, Topp E, Rosen J. 1990. An interactive graphics-based model of the lower extremity to study orthopedic surgical procedures. IEEE Trans Biomed Eng. 37:757–767.

Delp S, Loan J. 1995. A graphics-based software system to develop and analyze models of musculoskeletal structures. Comput Biol Med. 25:21–34.

Delp S, Anderson SC, Arnold AS, Loan P, Habib A, John CT, Guendelman E, Thelen DG. 1997. Opensim: Open-source software to create and analyze dynamic simulations of movement. IEEE Trans Biomed Eng. 54:1940–1950.

Dubousset J, Charpak G, Dorion I, Skalli W, Lavaste F, de Guise JA. 2005. A new 2D and 3D imaging approach to musculoskeletal physiology and pathology with low-dose radiation and the standing position: The EOS system. Bull Acad Natl Med. 189:287–297.

Eredmir A, McLean S, Herzog W, van den Bogert AJ. 2007. Model-based estimation of muscle forces exerted during movements. Clin Biomech. 22(2):131–154.

Heller M, Bergmann G, Deuretzbacher G, Dürselen L, Pohl M, Claes L, Haas N, Duda G. 2001. Musculo-skeletal loading conditions at the hip during walking and stair climbing. J Biomech. 34(7):883–893.

Jolivet E, Daguet E, Pomero V, Bonneau D, Laredo J, Skalli W. 2008. Volumic subject-specific reconstruction of muscular system based on a reduced dataset of medical images. Comput Methods Biomech Biomed Eng. 11(3):281–290.

Laporte S, Skalli W, de Guise JA, Lavaste F, Mitton D. 2003. A biplanar reconstruction method based on 2D and 3D contours: Application to the distal femur. Comput Methods Biomech Biomed Eng. 6(1):1–6.

Nordez A, Jolivet E, Südhoff I, Bonneau D, de Guise JA, Skalli W. 2009. Comparison of methods to assess quadriceps muscle volume using magnetic resonance imaging. J Magn Reson Imaging. 30(5):1116–1123.

Redl C, Gfoehler M, Pandy M. 2007. Sensitivity of muscle force estimates to variations in muscle-tendon properties. Hum Movement Sci. 26(2):306–319.

Reinbolt JA, Schutte JF, Fregly BJ, Koh BI, Haftka RT, George AD, Mitchell KH. 2005. Determination of patient-specific multi-joint kinematic models through two-level optimization. J Biomech. 38(3):621–626.

Scheys L, Spaepen A, Suetens P, Jonkers I. 2008. Calculated moment-arm and muscle-tendon lengths during gait differ substantially using MR based versus rescaled generic lower-limb musculoskeletal models. Gait Posture. 28(4):640–648.

Scheys L, Loeckx D, Spaepen A, Suetens P, Jonkers I. 2009. Atlas-based non-rigid image registration to automatically define line-of-action muscle models: A validation study. J Biomech. 42(5):565–572.

Scheys L, Desloovere K, Suetens P, Jonkers I. 2011. Level of subject-specific detail in musculoskeletal models affects hip moment arm length calculation during gait in pediatric

subjects with increased femoral anteversion. J Biomech. 44: 1346–1353.
Südhoff I, De Guise JA, Nordez A, Jolivet E, Bonneau D, Khoury V, Skalli W. 2009. 3D-subject-specific geometry of the muscles involved in knee motion from selected MRI images. Med Biol Eng Comput. 47:579–587.
Trochu F. 1993. A contouring program based on dual kriging interpolation. Eng Comput. 9:160–177.